Applied Physics Letters ARTICLE scitation.org/journal/apl

Interfacial modification mechanism by aging effect for high-performance Cd-free and all-dry process Cu(In,Ga)(S,Se)$_2$ solar cells

Cite as: Appl. Phys. Lett. **117**, 223501 (2020); doi: 10.1063/5.0031241
Submitted: 29 September 2020 · Accepted: 13 November 2020 ·
Published Online: 30 November 2020

Takahito Nishimura,[1,a)] Jakapan Chantana,[2,3] Yu Kawano,[3] Akira Yamada,[4] Yoshinori Kimoto,[5] Takuya Kato,[5] Hiroki Sugimoto,[5] and Takashi Minemoto[3,a)]

AFFILIATIONS

[1]Ritsumeikan Global Innovation Research Organization, Ritsumeikan University, 1-1-1 Nojihigashi, Kusatsu, Shiga 525-8577, Japan
[2]Research Organization of Science and Technology, Ritsumeikan University, 1-1-1 Nojihigashi, Kusatsu, Shiga 525-8577, Japan
[3]Department of Electrical and Electronic Engineering, Ritsumeikan University, 1-1-1 Nojihigashi, Kusatsu, Shiga 525-8577, Japan
[4]Department of Electrical and Electronic Engineering, Tokyo Institute of Technology, Meguro-ku, Tokyo 152-8552, Japan
[5]Advanced Technology Research Laboratories, Idemitsu Kosan Co., Ltd., Atsugi, Kanagawa 243-0206, Japan

[a)]**Authors to whom correspondence should be addressed:** nishi-tk@fc.ritsumei.ac.jp and minemoto@se.ritsumei.ac.jp

ABSTRACT

Modification of the hetero-junction interface in Cd-free and all-dry process Cu(In,Ga)(S,Se)$_2$ (CIGSSe) solar cells by introducing the aging process for the bare CIGSSe films is demonstrated, ultimately achieving the highest conversion efficiency of 22.0%. In this article, two positive effects of the aging process are discussed. First, additional phases, such as In$_x$(O,S)$_y$ and Cu-deficient phases, are naturally formed on the CIGSSe surface. Second, unintentional segregation of Zn-rich particles at the (Zn,Mg)O/CIGSSe interface during the (Zn,Mg)O deposition is suppressed. These effects lead to the reduction of recombination at the hetero-junction interface and dramatic enhancement of performance for the Cd-free and all-dry process CIGSSe solar cells.

Chalcopyrite compound materials, such as Cu(In,Ga)Se$_2$, Cu(In,Ga)(S,Se)$_2$ (CIGSSe), and Cu(In,Ga)S$_2$, are expected as promising photovoltaic materials since they can be applied for flexible light-weight solar cells, which realize high-speed and low-cost production. There are some reports that high efficiency over 20% in Cu(In,Ga)Se$_2$ solar cells was achieved by applying CdS as a traditional *n*-type buffer layer[1,2] fabricated by the chemical bath deposition (CBD) process.[3] However, alternative buffer incorporating no toxic Cd elements is desirable from a viewpoint of environmental problems. Therefore, a Cd-free Cu(In,Ga)Se$_2$ solar cell without CdS buffer has been developed to produce eco-friendly solar cells.[4] In particular, the record efficiency of 23.35% has been recently achieved in Cd-free CIGSSe solar cells using Zn(O,S,OH)$_x$ buffer fabricated by the CBD process.[5] Further reduction of production cost for CIGSSe solar cells can be expected if the industrial waste treatment is prevented by realizing the all-dry process without the CBD process. We have proposed the aging process[6] for the bare CIGSSe films to realize high-efficient Cd-free CIGSSe solar cells fabricated by the all-dry process. In this article, the modification mechanism at the (Zn,Mg)O/CIGSSe hetero-junction interface is discovered for the Cd-free and all-dry process CIGSSe solar cells completed by introducing the aging process, demonstrating the usefulness of the aging effect on device performance. The formation mechanism of additional phases, e.g., In$_x$(O,S)$_y$ and Cu-deficient phases, on the CIGSSe surface by the Na catalytic effect is revealed. Furthermore, the segregation process of Zn-rich particles at the (Zn,Mg)O/CIGSSe interface is discussed, suggesting that the aging process is effective in preventing the unintentional formation of Zn-rich segregation.

Cd-free CIGSSe solar cells with a stacked structure with Al/Ni/ (B- or Al-doped (Zn,Mg)O)/i-(Zn,Mg)O/CIGSSe/Mo/glass were fabricated. The *p*-type CIGSSe films were fabricated by sputtering an In/Cu–Ga metal precursor on the Mo-coated glass substrate followed by the sulfurization after selenization (SAS) process. Further detailed information on the fabrication process has been discussed elsewhere.[7–10] A CsF layer with a thickness of 3–15 nm was deposited on the CIGSSe surface and then annealed at a temperature of 250–350 °C.[11] In this work, the aging process was introduced after the fabrication of the CsF-treated CIGSSe films,[6] which were kept in a desiccator cabinet under a back

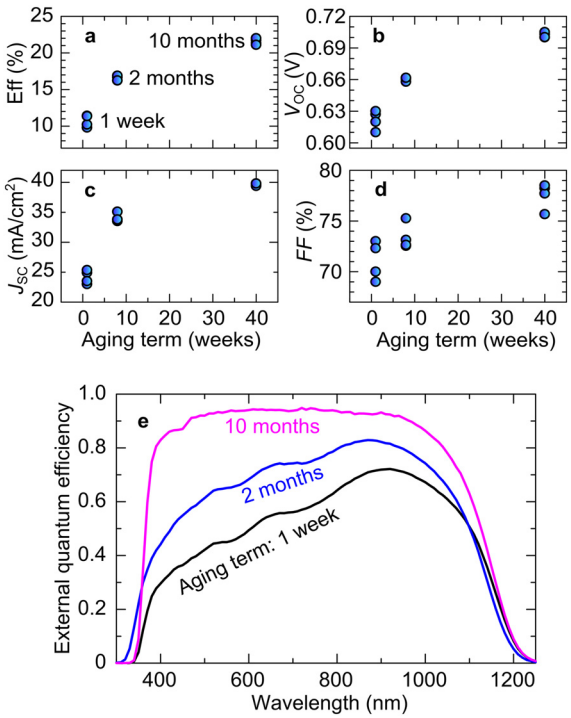

FIG. 1. (a) Conversion efficiency, (b) V_{OC}, (c) J_{SC}, and (d) *FF*, and (e) EQE for Cd-free and all-dry process CIGSSe solar cells with the aging process of 1 week, 2 months, and 10 months.

pressure of approximately 1.0×10^3 Pa with a partial pressure for oxygen of approximately 200 Pa for the term from 1 week to 2 years. Then, without any CIGSSe surface cleaning, an intrinsic (Zn,Mg)O layer with a thickness of approximately 150 nm was deposited[9] on CIGSSe films at room temperature by a radio frequency (RF) magnetron co-sputtering system. The sputtering power of 82.6 and 85.0 W was induced to the ZnO and MgO targets of 99.99% purity with a target diameter of 7.62 cm. The background pressure before the deposition was 2.0×10^{-4} Pa. The Ar gas flow rate and working pressure were adjusted to 3.9 sccm and 0.1 Pa, respectively. The compositional ratio of Mg/(Mg + Zn) was controlled to be approximately 0.2. As an *n*-type transparent conductive oxide layer, Al-doped (Zn,Mg)O or B-doped (Zn,Mg)O layers with a Mg/(Mg + Zn) ratio of about 0.1 were deposited. An Al-doped (Zn,Mg)O layer with a thickness of approximately 800 nm was deposited at room temperature by a RF magnetron co-sputtering system using Al-doped ZnO (AZO) (Al_2O_3: 2 wt. %-doped) and MgO targets of 99.99% purity.[12,13] B-doped (Zn,Mg)O layer with a thickness of approximately 1000 nm was deposited[14] at a substrate temperature of 185 °C by a metal organic chemical vapor deposition system. 100 nm-thick Ni and 4000 nm-thick Al grid-electrodes were deposited by an electron beam evaporation system. An anti-reflection coating layer was not applied. Finally, heat-light soaking and light soaking processes were performed[15] for the completed Cd-free and all-dry process CIGSSe solar cells.

The current density–voltage (*J*–*V*) response and external quantum efficiency (EQE) for the CIGSSe solar cells were measured under AM1.5G equivalent irradiation (100 mW/cm^2) at room temperature. Saturation current density (J_0), ideality factor (*n*), series resistance (R_s), and shunt resistance (R_{sh}) were estimated by fitting the *J*–*V* curves using the one-diode model. A cross section of the CIGSSe solar cells was analyzed by an electron beam-induced current (EBIC) measurement, which was employed by a field emission scanning electron microscope (JEOL JSM-7001F). The elemental composition for the cross section of the CIGSSe solar cells was analyzed by an energy dispersive x-ray spectrometry (EDX) system (JEOL JED-2300T) installed on a scanning transmission electron microscope (STEM) (JEOL JEM-ARM200F). The surface composition of the CIGSSe films was analyzed by an x-ray photoelectron spectroscopy (XPS) system (PHI Quantera II), where the information depth is below 5 nm.

Figure 1 depicts the (a) conversion efficiency, (b) open-circuit voltage (V_{OC}), (c) short-circuit current density (J_{SC}), (d) fill factor (*FF*), and (e) EQE spectrum for the Cd-free and all-dry process CIGS solar cells. Table I shows the mean values and standard deviation of conversion efficiency, V_{OC}, J_{SC}, and *FF* in the aging term of 1 week, 2 months, and 10 months. Four samples were prepared for each aging condition. Mean values of conversion efficiency, V_{OC}, J_{SC}, and *FF* were clearly improved from 10.7%, 0.622 V, 24.2 mA/cm^2, and 71.1% to 21.5%, 0.702 V, 39.6 mA/cm^2, and 77.5%, respectively, with the increasing aging term from 1 week to 10 months. One-diode parameters of J_0, *n*, R_s, and R_{sh} for the best-cell are also shown in Table I. J_0 and *n* were reduced from 4.8×10^{-9} A/cm^2 and 1.57 at 1 week to 1.0×10^{-10} A/cm^2 and 1.38 at 10 months, relating to the reduction of minority carrier recombination in the devices. EQE in the short wavelength region of 350–900 nm was notably improved with the aging term, leading to the enhancement of J_{SC}. Figure 2 depicts (a), (c), and (e) back-scattered electron (BSE) images and (b), (d), and (f) EBIC mappings for the cross section of the CIGSSe solar cells. Intensity of EBIC signals in the CIGSSe region near the (Zn,Mg)O/CIGSSe interface was clearly enhanced, and the region with a high EBIC signal (green-colored) was widened into the CIGS bulk side with increasing the aging term from 1 week to 10 months. This result suggests that the carrier collection length was improved by reducing carrier recombination around the (Zn,Mg)O/CIGSSe interface with the

TABLE I. Mean value and standard deviation of conversion efficiency, V_{OC}, J_{SC}, and *FF*, as well as one-diode parameters of J_0, *n*, R_s, and R_{sh} in the best device for the Cd-free and all-dry process CIGSSe solar cells with the aging process of 1 week, 2 months, and 10 months.

Aging term	Eff. (%)	V_{OC} (V)	J_{SC} (mA/cm^2)	*FF* (%)	J_0 (A/cm^2)	*n*	R_S (Ω cm^2)	R_{Sh} (Ω cm^2)
1 Week	10.7 ± 0.8	0.622 ± 0.009	24.2 ± 1.1	71.1 ± 1.9	4.8×10^{-9}	1.57	0.969	1260
2 Months	16.5 ± 0.3	0.660 ± 0.002	34.0 ± 0.7	73.4 ± 1.3	5.5×10^{-10}	1.43	0.650	1060
10 Months	21.5 ± 0.4	0.702 ± 0.002	39.6 ± 0.2	77.5 ± 1.3	1.0×10^{-10}	1.38	0.235	910

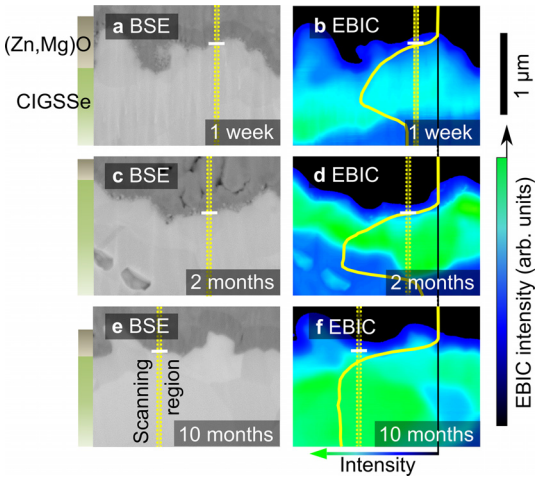

FIG. 2. (a), (c), and (e) BSE images and (b), (d), and (f) EBIC mappings for Cd-free and all-dry process CIGSSe solar cells with the aging process of 1 week, 2 months, and 10 months.

aging process, leading to the enhancement of the short wavelength response in EQE as well as improved J_{SC} and V_{OC}. Finally, the highest conversion efficiency of 22.0% was achieved for the 10-month sample, which has a V_{OC} of 0.705 V, a J_{SC} of 39.8 mA/cm^2, and a *FF* of 78.5% as shown in Fig. 3.

Figure 4 shows (a), (b), and (c) STEM images and (d), (e), and (f) EDX mappings of Zn elements for the cross section of the CIGSSe solar cells. For 1-week and 2-month samples, particles with the diameter of 10–30 nm were formed at the (Zn,Mg)O/CIGSSe interface as shown in Figs. 4(a) and 4(b), whereas those were not observed for the 10-month samples in Fig. 4(c). In Figs. 4(d) and 4(e), high Zn contents were observed at the particles in 1-week and 2-month samples. To quantitatively discuss the composition, point analysis by

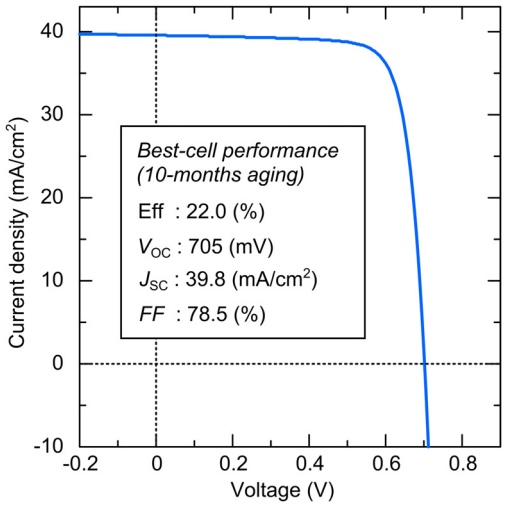

FIG. 3. *J–V* characteristics for the highest-efficiency CIGSSe solar cell with the aging process of 10 months.

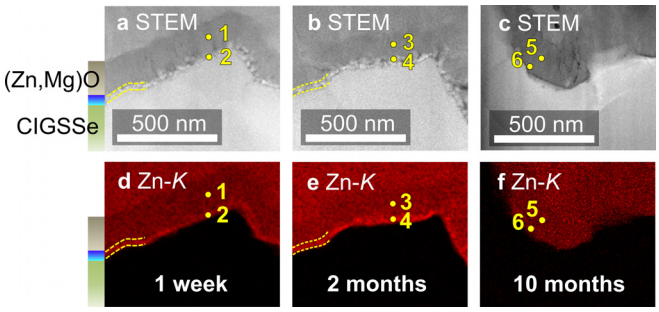

FIG. 4. (a), (c), and (e) STEM images and (b), (d), and (f) EDX mappings for Cd-free and all-dry process CIGSSe solar cells with the aging process of 1 week, 2 months, and 10 months.

TEM–EDX was performed at the points of 1–6 in Fig. 4. This result is summarized in Table II. For the 1-week and 2-month samples, the Zn content of 66.4 and 67.7 at. % was detected at points 2 and 4 in the particles, which was much higher than that of 48.9 and 45.8 at. % at points 1 and 3 in the (Zn,Mg)O region. For the 10-month sample, Zn contents of 44.2 and 48.2 at. % in the (Zn,Mg)O region were comparable at points 5 and 6 in the center and near the interface with CIGSSe, respectively. These results suggest that, for the short aging samples, the Zn-rich particles were unintentionally segregated during the (Zn,Mg)O deposition, leading to the carrier recombination near the (Zn,Mg)O/CIGSSe interface [Figs. 2(b) and 2(d)].

Figure 5 depicts the XPS spectrum of (a) Cu $2p_{3/2}$, (b) In $3d_{5/2}$, (c) Ga $2p_{3/2}$, and (d) S $2p$ for the surface of the bare CIGSSe films on a Mo-coated glass substrate with the aging term of 1 week and 2 years. The 2-year sample was used to clearly examine the aging effect. Table III shows the surface composition quantitatively estimated by XPS analysis. The Cu content and Cu/(Ga + In) ratio in the 2-year sample were 8.0 at. % and 0.32, respectively, which were lower than those of 19.0 at. % and 0.57 for the 1-week sample. It should be noted that the 2-year sample had a high Na content of 39.2 at. % near the surface of the CIGSSe surface although the 1-week sample had that of 9.9 at. %, suggesting that the Na element is diffused out from the rear of the CIGSSe, at which the Na element is mostly accumulated in the as-deposited CIGSSe.[11]

In our previous study, it was found that $In_x(O,S)_y$ compounds, such as In(O,S) and $In_2(O,S)_3$, were formed on the CIGSSe surface with the aging process.[6] So far, the model of the Na catalytic effect for oxidation of $Cu(In,Ga)Se_2$ has been suggested.[16] Na is related to the polarization of the O–O bond in the physisorbed O_2 molecule and the formation of O_2^-, resulting in the In–O bond because of thermodynamic driving force. Therefore, it is considered that, in the two-year sample, the increased Na content (Table III) accelerated oxidation of the CIGSSe surface and formation of $In_x(O,S)_y$ compounds. In addition, it has been reported that surface oxidation by the Na catalytic effect leads to reduction of the Cu content in $Cu(In,Ga)Se_2$.[17,18] The In–O bond formed in the CIGSSe crystal is highly polarized owing to the different electronegativities of 1.7 and 3.5 for In and O, respectively, leading to the increase in the ionic nature for the In–S bond and making the S atom more negative. Finally, covalent nature of the Cu–S bond is weakened, tending to release the Cu atom from the site. In Table III, the Cu/(Ga + In) ratio was actually decreased from 0.57 to

TABLE II. Cross-sectional composition analyzed by TEM equipped with EDX near the interface between (Zn,Mg)O and CIGSSe for Cd-free and all-dry process CIGSSe solar cells with the aging term of 1 week, 2 months, and 10 months. The positions at points of 1–6 analyzed by the TEM–EDX measurement are indicated in Fig. 4.

			Composition (at. %)						
Aging term	Point no.	Analyzed region	Cu	In	Ga	S	Zn	Mg	O
1 Week	1	(Zn,Mg)O	0.0	0.1	0.2	0.1	48.9	10.9	42.6
	2	Particles	1.0	4.3	0.4	5.2	66.4	2.7	20.0
2 Months	3	(Zn,Mg)O	0.0	0.1	0.2	0.1	45.8	13.0	41.8
	4	Particles	0.2	3.8	0.4	3.4	67.7	1.0	23.4
10 Months	5	(Zn,Mg)O	0.1	0.0	0.1	0.0	44.2	8.0	48.4
	6	Interface [(Zn,Mg)O side]	0.2	0.2	0.2	0.3	48.2	8.4	42.5

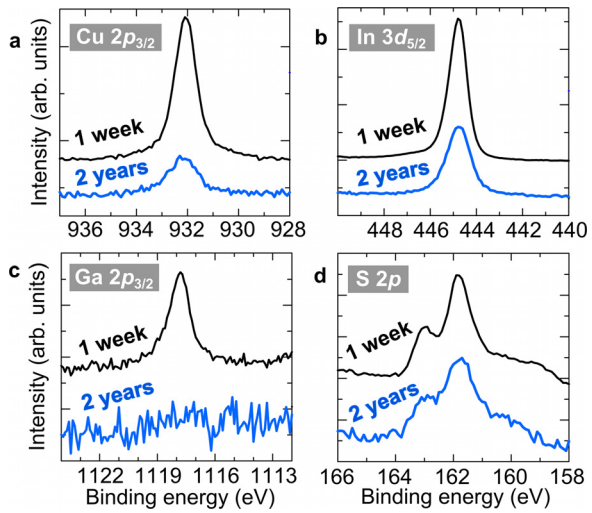

FIG. 5. XPS spectrum of (a) Cu $2p_{3/2}$, (b) In $3d_{5/2}$, (c) Ga $2p_{3/2}$, and (d) S $2p$ for the surface of the CIGSSe films on the Mo-coated glass substrate with the aging process of 1 week and 2 years.

0.32 with the aging term from 1 week to 2 years. We concluded that the $In_x(O,S)_y$ and Cu-deficient phases are naturally formed on the CIGSSe surface owing to the Na catalytic effect by the aging process. It has been reported that $In_x(O,S)_y$ has been applied for a buffer layer to adjust the conduction band alignment and form a hole barrier by the valence band offset at the hetero-interface for the $Cu(In,Ga)Se_2$ solar cells.[19] Additionally, Cu-deficient phases, such as $Cu(In,Ga)_3Se_5$ with the Cu/(Ga + In) ratio of 0.33, act as hole blocking layer, resulting in the reduction of recombination owing to carrier separation by forming the valence band offset at the hetero-interface.[20–24] Hence, the $In_x(O,S)_y$ and Cu-deficient phases naturally formed on the CIGSSe surface by the aging process reduced carrier recombination at the (Zn,Mg)O/CIGSSe hetero-interface as shown in the EBIC mappings (Fig. 2).

TABLE III. Surface composition estimated by the XPS measurement for the CIGSSe films on the Mo-coated glass substrate with the aging process of 1 week and 2 years.

	Composition (at. %)					
Aging term	Cu	In	Ga	S	Na	Cu/(Ga + In)
1 Week	19.0	31.0	2.6	37.5	9.9	0.57
2 Years	8.0	25.4	0	27.4	39.2	0.32

In Fig. 4, the Zn-rich particles were observed at the (Zn,Mg)O/CIGSSe interface in 1-week and 2-month samples and diminished in the 10-month sample. The stable existence of NaOH or Na_2SeO_3 in a few-nm region near the $Cu(In,Ga)Se_2$ outermost surface has been reported.[25] In our sputtering system, the substrate temperature during the (Zn,Mg)O deposition is unintentionally elevated to 80–85 °C owing to induced sputtering power. In the short-aging term of 1 week, although the Na content on the bare CIGSSe surface is lower (Table III), it is considered that Na compounds, e.g., NaOH or $Na_2(S,Se)O_3$, are segregated on the surface during the (Zn,Mg)O deposition because of Na diffusion accelerated by substrate heating. The NaOH–ZnO chemical reaction has been used for the crystal growth of ZnO,[26] structural control of crystal ZnO by the chemical etching,[27,28] or pretreatment for metal plating (Zincate treatment[29]). For this reaction system, control of pH in NaOH solution is important, relating to the ZnO solubility depending on Zn species [e.g., Zn^{2+}, $Zn(OH)^+$, $Zn(OH)_20$, $Zn(OH)_3^-$, and $Zn(OH)_4^{2-}$].[26] In short-aging samples, it is speculated that (Zn,Mg)O is dissolved by NaOH or $Na_2(S,Se)O_3$ during the initial step of its deposition, re-growing Zn-rich particles as shown in Figs. 4(a), 4(d), 4(b), and 4(e). On the other hand, for long-aging samples, NaOH or $Na_2(S,Se)O_3$ absorbs H_2O from ambient with an oxygen partial pressure of approximately 200 Pa in a desiccator cabinet during the aging term, resulting in that pH on the CIGSSe outermost surface is close to neutral (pH = 7). Therefore, by introducing a sufficient aging term of 10 months, dissolution of (Zn,Mg)O is suppressed, finally eliminating the segregation of Zn-rich particles [Figs. 4(c) and 4(f)]. It has been reported that the performance of the $CdS/Cu(In,Ga)Se_2$ solar cells is improved by Na doping owing to diffusion from the soda-lime glass or deposited NaF precursor,[30,31] while Na incorporation leads to performance degradation for the $ZnO/Cu(In,Ga)Se_2$ structure without CBD–CdS buffer.[32] In our study, despite the increase in the Na content with the aging process on the CIGSSe surface (Table III) in the (Zn,Mg)O/CIGSSe structure without CBD–CdS buffer, device performance was drastically improved (Fig. 1 and Table I). This is due to the elimination of (Zn,Mg)O dissolution, improving carrier collection near the

(Zn,Mg)O/CIGSSe hetero-junction interface (Fig. 2). Finally, the highest conversion efficiency of 22.0% was achieved by the aging effect of 10 months for the Cd-free and all-dry process CIGSSe solar cells owing to the self-formation of $In_x(O,S)_y$ and Cu-deficient phases and elimination of segregated Zn-rich particles. The development of techniques to accelerate the aging effect for a shorter term is required in a future work.

In summary, the mean conversion efficiency was clearly improved from 10.7% to 21.5% by increasing the aging term from 1 week to 10 months for CIGSSe solar cells. Two positive effects of the aging process led to the improvement of device performance. First, additional phases such as $In_x(O,S)_y$ and Cu-deficient phases were naturally formed on the CIGSSe surface due to the Na catalytic effect, leading to the reduction of carrier recombination because of the desirable valence band alignment near the hetero-junction interface. Second, segregation of Zn-rich particles at the (Zn,Mg)O/CIGSSe interface was suppressed by preventing (Zn,Mg)O dissolution since Na compounds, e.g., NaOH or $Na_2(S,Se)O_3$, absorb H_2O from ambient during the aging term. Ultimately, the highest conversion efficiency of 22.0% was achieved by applying the aging process for the Cd-free CIGSSe solar cells completed by the all-dry process.

This work was supported by the New Energy and Industrial Technology Development Organization (NEDO) under the Ministry of Economy, Trade and Industry.

DATA AVAILABILITY

The data that support the findings of this study are available from the corresponding author upon reasonable request.

REFERENCES

[1]A. Chirilă, P. Reinhard, F. Pianezzi, P. Bloesch, A. R. Uhl, C. Fella, L. Kranz, D. Keller, C. Gretener, H. Hagendorfer, D. Jaeger, R. Erni, S. Nishiwaki, S. Buecheler, and A. N. Tiwari, Nat. Mater. **12**, 1107 (2013).
[2]P. Jackson, D. Hariskos, R. Wuerz, O. Kiowski, A. Bauer, T. M. Friedlmeier, and M. Powalla, Phys. Status Solidi-Rapid Res. Lett. **9**, 28 (2015).
[3]Y. Hashimoto, N. Kohara, T. Negami, N. Nishitani, and T. Wada, Sol. Energy Mater. Sol. Cells **50**, 71 (1998).
[4]D. Hariskos, S. Spiering, and M. Powalla, Thin Solid Films **480-481**, 99 (2005).
[5]M. Nakamura, K. Yamaguchi, Y. Kimoto, Y. Yasaki, T. Kato, and H. Sugimoto, IEEE J. Photovoltaics **9**, 1863 (2019).
[6]J. Chantana, T. Nishimura, Y. Kawano, N. Suyama, A. Yamada, Y. Kimoto, T. Kato, H. Sugimoto, and T. Minemoto, Adv. Energy Mater. **9**, 1902869 (2019).
[7]K. Kushiya, T. Kase, T. Tachiyuki, I. Sugiyama, Y. Satoh, M. Satoh, and H. Takeshita, in Proceedings of the 25th IEEE Photovoltaic Specialists Conference (1996), p. 989.
[8]S. Niki, M. Contreras, I. Repins, M. Powalla, K. Kushiya, S. Ishizuka, and K. Matsubara, Prog. Photovoltaics: Res. Appl. **18**, 453 (2010).
[9]J. Chantana, T. Kato, H. Sugimoto, and T. Minemoto, Prog. Photovoltaics: Res. Appl. **25**, 431 (2017).
[10]K. Takuya, Jpn. J. Appl. Phys., Part 1 **56**, 04CA02 (2017).
[11]T. Kato, A. Handa, T. Yagioka, T. Matsuura, K. Yamamoto, S. Higashi, J.-L. Wu, K. F. Tai, H. Hiroi, T. Yoshiyama, T. Sakai, and H. Sugimoto, IEEE J. Photovoltaics **7**, 1773 (2017).
[12]J. Chantana, T. Kato, H. Sugimoto, and T. Minemoto, Prog. Photovoltaics: Res. Appl. **25**, 996 (2017).
[13]T. Nishimura, S. Kim, J. Chantana, Y. Kawano, S. Ishizuka, and T. Minemoto, Sol. Energy Mater. Sol. Cells **202**, 110157 (2019).
[14]J. Chantana, Y. Kawano, T. Nishimura, T. Kato, H. Sugimoto, and T. Minemoto, Sol. Energy **184**, 553 (2019).
[15]J. Chantana, T. Kato, H. Sugimoto, and T. Minemoto, Prog. Photovoltaics: Res. Appl. **26**, 868 (2018).
[16]L. Kronik, D. Cahen, and H. W. Schock, Adv. Mater. **10**, 31 (1998).
[17]U. Rau, D. Braunger, R. Herberholz, H. W. Schock, J. F. Guillemoles, L. Kronik, and D. Cahen, J. Appl. Phys. **86**, 497 (1999).
[18]L. Kronik, U. Rau, J. F. Guillemoles, D. Braunger, H. W. Schock, and D. Cahen, Thin Solid Films **361-362**, 353 (2000).
[19]W. Ho, C. Hsu, S. Wei, C. Cai, W. Huang, and C. Lai, ACS Appl. Mater. Interfaces **9**, 17586 (2017).
[20]T. Nishimura, K. Nakada, and A. Yamada, ACS Appl. Energy Mater. **2**, 5103 (2019).
[21]T. Nishimura, H. Sugiura, K. Nakada, and A. Yamada, Prog. Photovoltaics: Res. Appl. **27**, 171 (2019).
[22]T. Nishimura, S. Toki, H. Sugiura, K. Nakada, and A. Yamada, Prog. Photovoltaics: Res. Appl. **26**, 291 (2018).
[23]T. Nishimura, H. Sugiura, K. Nakada, and A. Yamada, Phys. Status Solidi-Rapid Res. Lett. **12**, 1800129 (2018).
[24]T. Nishimura, S. Toki, H. Sugiura, K. Nakada, and A. Yamada, Appl. Phys. Express **9**, 092301 (2016).
[25]D. W. Niles, K. Ramanathan, F. Hasoon, R. Noufi, B. J. Tielsch, and J. E. Fulghum, J. Vac. Sci. Technol., A **15**, 3044 (1997).
[26]R. B. Peterson, C. L. Fields, and B. A. Gregg, Langmuir **20**, 5114 (2004).
[27]Y. Wang, Y. Gu, S. Peng, W. Ding, H. Wang, and W. Chai, Appl. Surf. Sci. **257**, 8044 (2011).
[28]J. Zhou, N. S. Xu, and Z. L. Wang, Adv. Mater. **18**, 2432 (2006).
[29]F. Keller and W. G. Zelley, J. Electrochem. Soc. **97**, 143 (1950).
[30]M. A. Contreras, B. Egaas, P. Dippo, J. Webb, J. Granata, K. Ramanathan, S. Asher, A. Swartzlander, and R. Noufi, in Proceedings of the 27th IEEE Photovoltaic Specialists Conference (1997), p. 359.
[31]R. Caballero, C. A. Kaufmann, T. Eisenbarth, T. Unold, S. Schorr, R. Hesse, R. Klenk, and H. W. Schock, Phys. Status Solidi **206**, 1049 (2009).
[32]L. Kronik, B. Mishori, E. Fefer, Y. Shapira, and W. Riedl, Sol. Energy Mater. Sol. Cells **51**, 21 (1998).